Electronic Supplementary Material (ESI) for Dalton Transactions.
This journal is © The Royal Society of Chemistry 2022

Electronic Supporting Information

Ni(II) complexes of a new asymmetric tetradentate NN'N''O picolinoyl-1,2-phenylenediamide-phenolate redox-active ligand in different redox levels

Narottam Mukhopadhyay, Arunava Sengupta, Aswin Kottapurath Vijay, Francesc Lloret and Rabindranath Mukherjee*

Figures:

Fig. S1 ^{1}H NMR ($CDCl_3$, 500 MHz) spectrum of H_3L^2.

Fig. S2 ^{13}C NMR ($CDCl_3$, 500 MHz) spectrum of H_3L^2.

Fig. S3 IR (in KBr) spectrum of H_3L^2.

Fig. S4 ESI-MS spectrum of H_3L^2.

Fig. S5 ESI-MS spectrum of $[Ni^{II}(L^2)]$ **1**.

Fig. S6 ESI-MS spectrum of $[Ni^{II}(L^2)](SbF_6)$ $\mathbf{1}^+$ / **2**.

Fig. S7 ESI-MS spectrum of $[Co(\eta^5\text{-}C_5H_5)_2][Ni^{II}(L^2)]$ $\mathbf{1}^-$ / **3**.

Fig. S8 Cyclic voltammogram of **2** in CH_2Cl_2.

Fig. S9 Cyclic voltammogram of **3** in CH_2Cl_2.

Fig. S10 ^{1}H NMR ($CDCl_3$, 500 MHz) spectrum of **2**.

Fig. S11 ^{1}H NMR ($CDCl_3$, 500 MHz) spectrum of **3**.

Fig. S12 Perspective view of H_3L^2 (both PART 1 and PART 2).

Fig. S13 Formation of alternating chains through π-π contacts in **1**•CH_3CN.

Fig. S14 X-band EPR spectra for **1** as solid recorded at (*a*) 300 K and (*b*) 80 K, along with their simulated versions.

Fig. S15 NIR region plot of (*a*) **1** and (*b*) **2** and their respective Gaussian-fit plot.

Fig. S16 TD-DFT-calculated electronic spectrum for $[Ni^{II}\{(L^2)^{\bullet 2-}\}]$ (**1**).

Fig. S17 Representative molecular-orbitals involved in TD-DFT transitions for $[Ni^{II}\{(L^2)^{\bullet 2-}]$ (**1**).

Fig. S18 TD-DFT-calculated electronic spectrum for $[Ni^{II}\{(L^2)^{-}\}]^+$ / $\mathbf{1}^+$.

Fig. S19 Representative molecular-orbitals involved in TD-DFT transitions for $[Ni^{II}\{(L^2)^{-}\}]^{+}$ / **1**$^{+}$.

Fig. S20 TD-DFT-calculated electronic spectrum for $[Ni^{II}\{(L^2)^{3-}]^{-}$ / **1**$^{-}$.

Fig. S21 Representative molecular-orbitals involved in TD-DFT transitions for $[Ni^{II}\{(L^2)^{3-}]^{-}$ / **1**$^{-}$.

Tables:

Table S1 Data collection and structure refinement parameters for H_3L^2 and $[Ni(L^2)]\bullet CH_3CN$ (**1**).

Table S2 Data collection and structure refinement parameters for $[Ni(L^2)](SbF_6)\bullet 0.5CH_2Cl_2$ (**2**$\bullet 0.5CH_2Cl_2$) and $[Co(\eta^5\text{-}C_5H_5)_2][Ni(L^2)]\bullet C_6H_6$ (**3**$\bullet C_6H_6$).

Table S3 Bond angles for $[Ni(L^2)]\bullet CH_3CN$ (**1**), $[Ni(L^2)](SbF_6)\bullet 0.5CH_2Cl_2$ (**2**$\bullet 0.5CH_2Cl_2$) and $[Co(\eta^5\text{-}C_5H_5)_2][Ni(L^2)]\bullet C_6H_6$ (**3**$\bullet C_6H_6$).

Table S4 Geometry-optimised cartesian coordinates for $[Ni(L^2)]$.

Table S5 Geometry-optimised cartesian coordinates for $[Ni(L^2)]^{+}$.

Table S6 Geometry-optimised cartesian coordinates for $[Ni(L^2)]^{-}$.

Table S7 DFT-calculated metric parameters for $[Ni(L^2)]$, $[Ni(L^2)]^{+}$ and $[Ni(L^2)]^{-}$.

Table S8 TD-DFT-calculated absorption spectral result for $[Ni(L^2)]$.

Table S9 TD-DFT-calculated absorption spectral result for $[Ni(L^2)]^{+}$.

Table S10 TD-DFT-calculated absorption spectral result for $[Ni(L^2)]^{-}$.

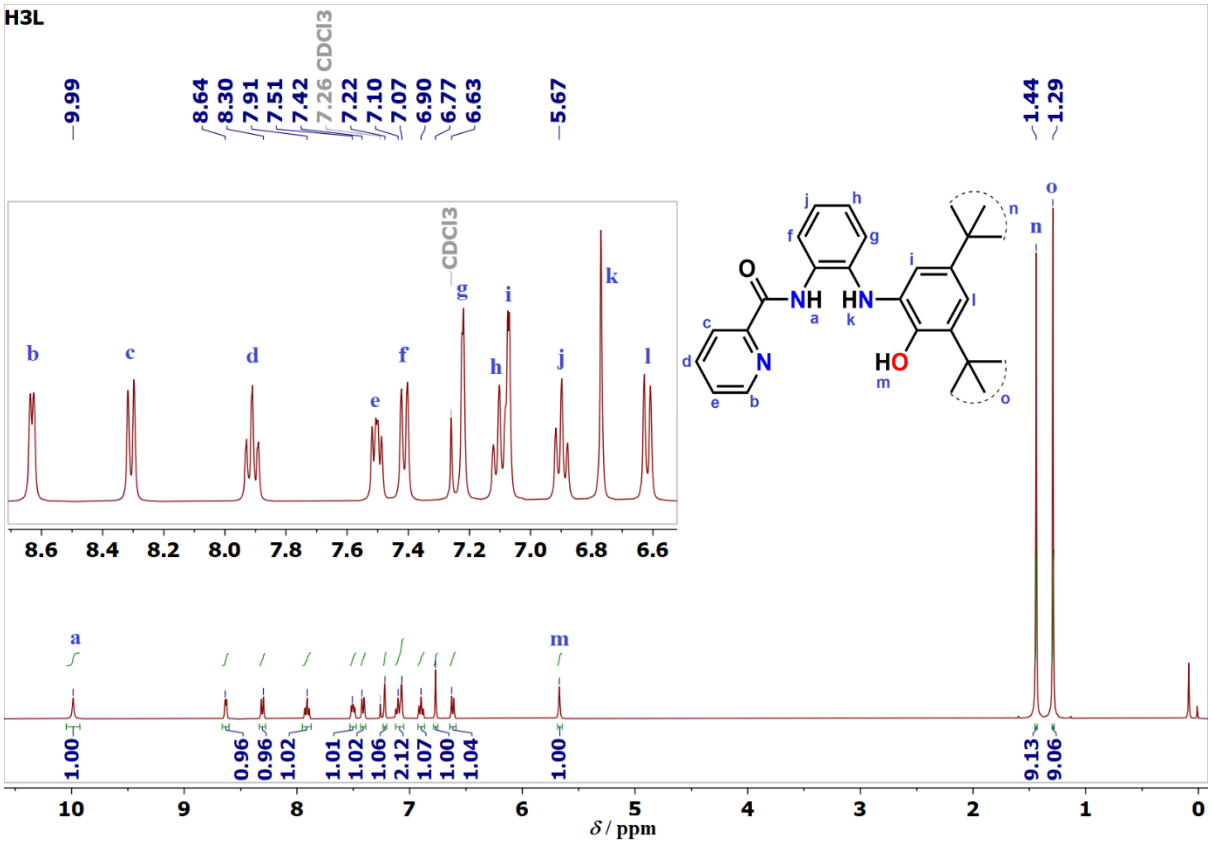

Fig. S1 ^{1}H NMR ($CDCl_3$, 500 MHz) spectrum of H_3L^2.

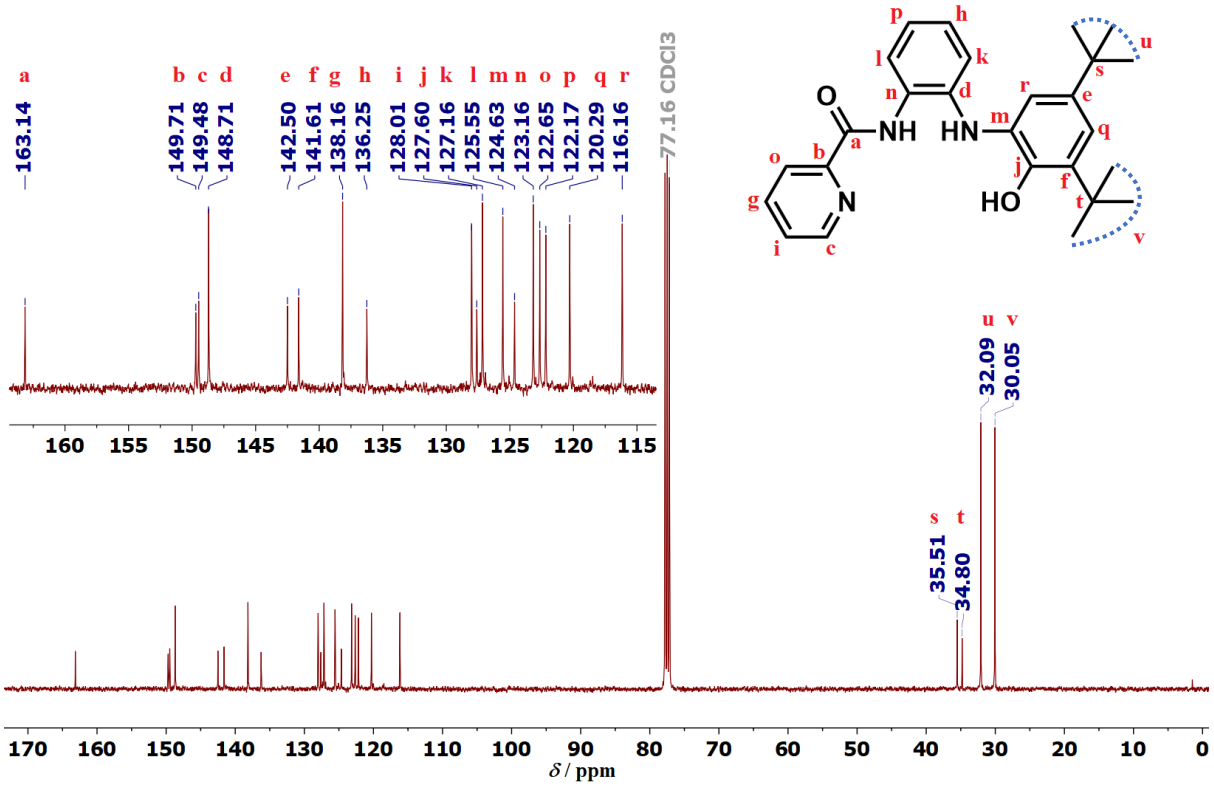

Fig. S2 ^{13}C NMR ($CDCl_3$, 500 MHz) spectrum of H_3L^2.

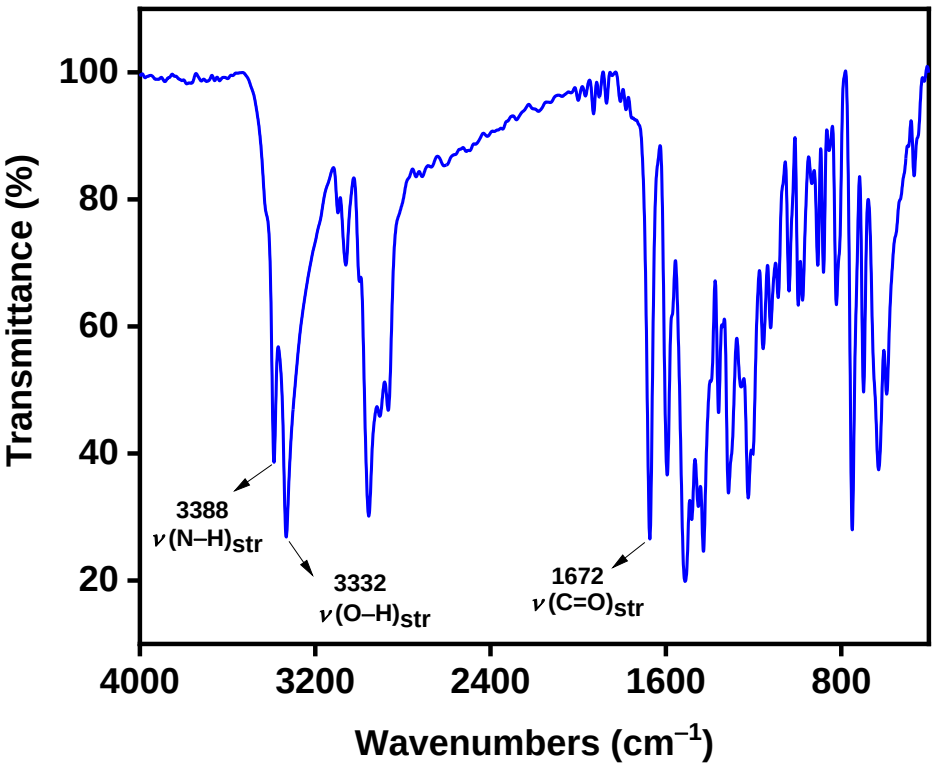

Fig. S3 IR (in KBr) spectrum of H_3L^2.

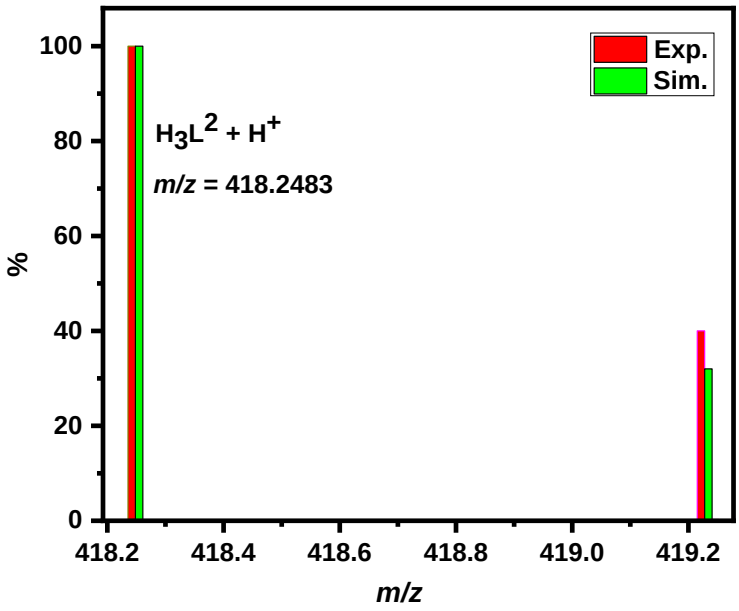

Fig. S4 Positive-ion ESI-MS spectra of H_3L^2 {$H_3L^2 + H^+$}.

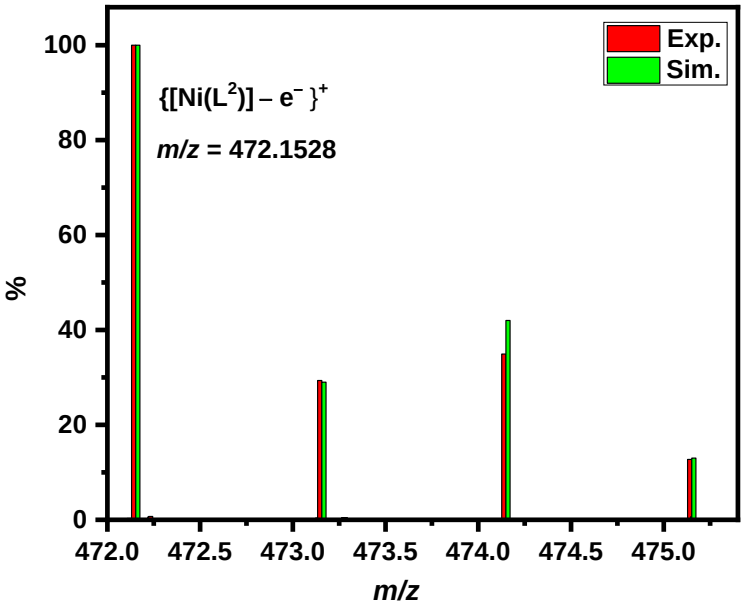

Fig. S5 Positive-ion ESI-MS spectrum of **1** / {[Ni(L^2)] – e^-}$^+$.

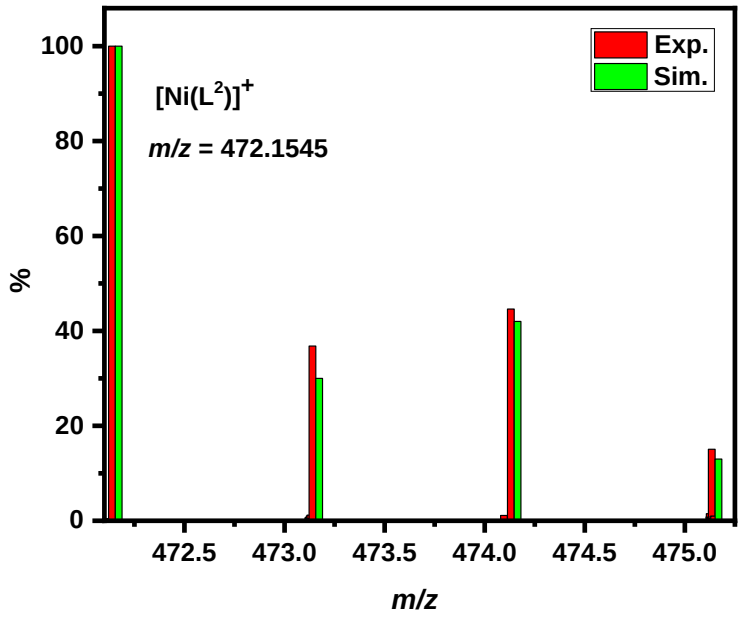

Fig. S6 Positive-ion ESI-MS spectrum of **2** / $[Ni(L^2)]^+$.

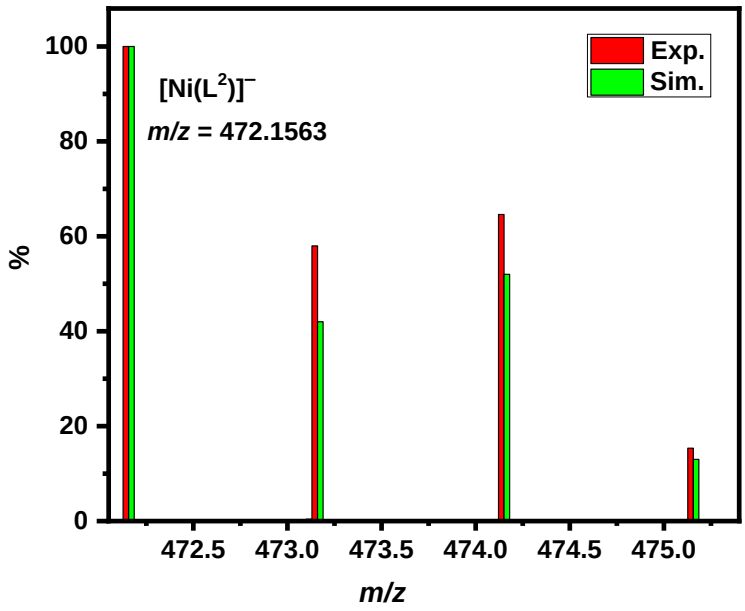

Fig. S7 Negative-ion ESI-MS spectrum of **3** / $\{[Ni(L^2)]^-$.

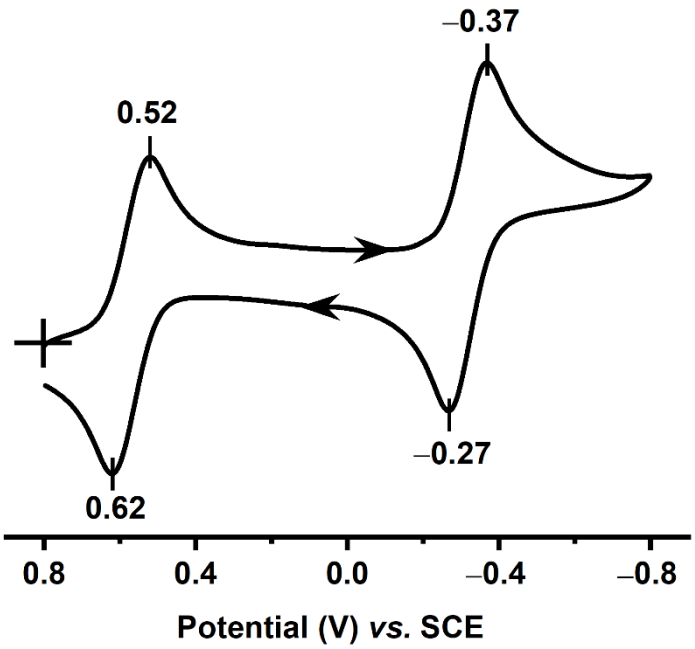

Fig. S8 Cyclic voltammogram of a 1.0 mM solution of **2** in CH_2Cl_2 (0.1 M TBAP supporting electrolyte; scan rate 100 mVs^{-1}; Pt working electrode) at 298 K.

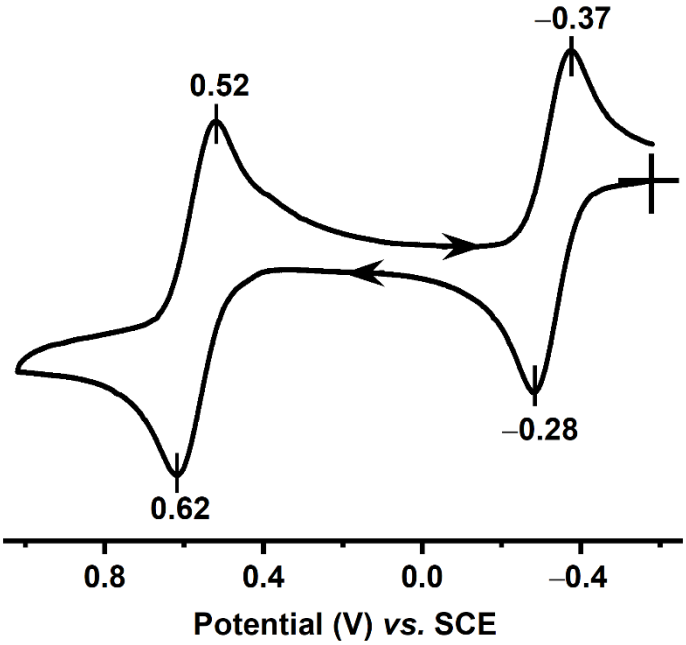

Fig. S9 Cyclic voltammogram of a 1.0 mM solution of **3** in CH_2Cl_2 (0.1 M TBAP supporting electrolyte; scan rate 100 mVs^{-1}; Pt working electrode) at 298 K.

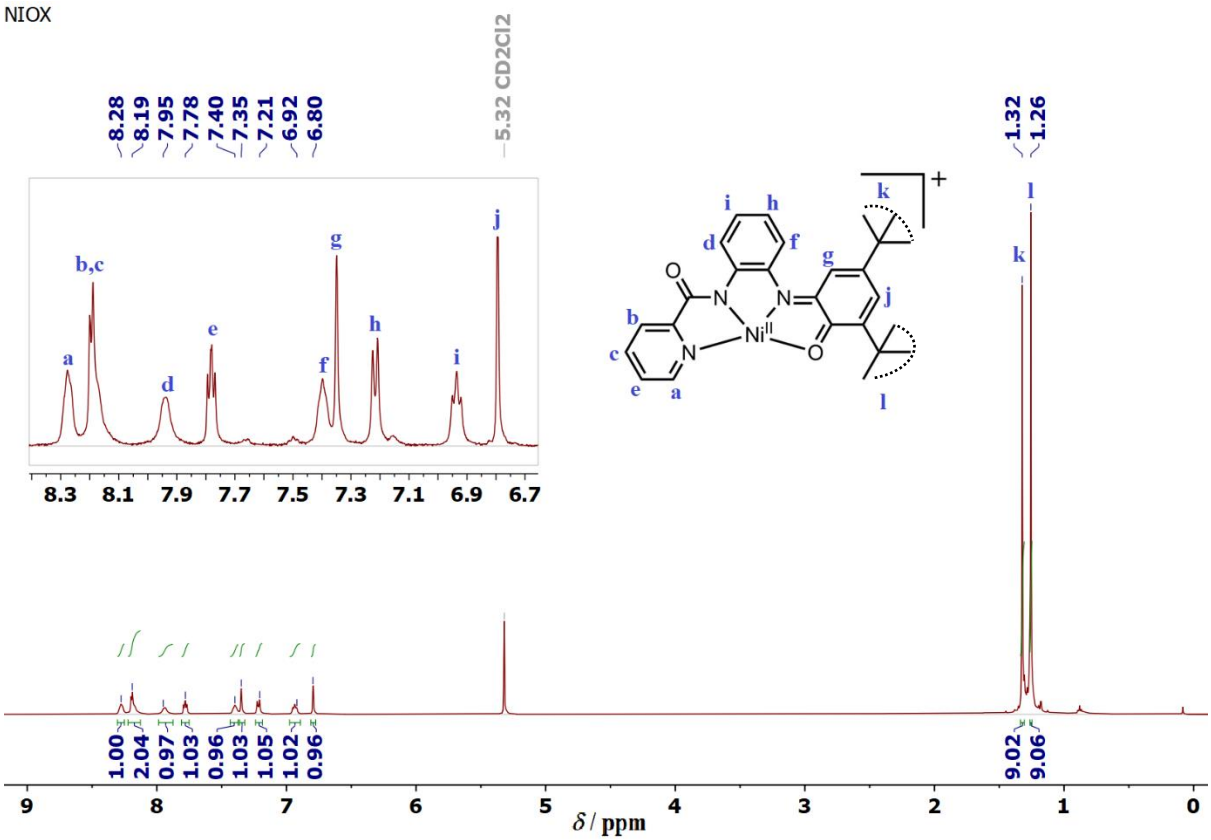

Fig. S10 ^{1}H NMR (CD_2Cl_2, 500 MHz) spectrum of [Ni(L^2)](SbF_6) **2**.

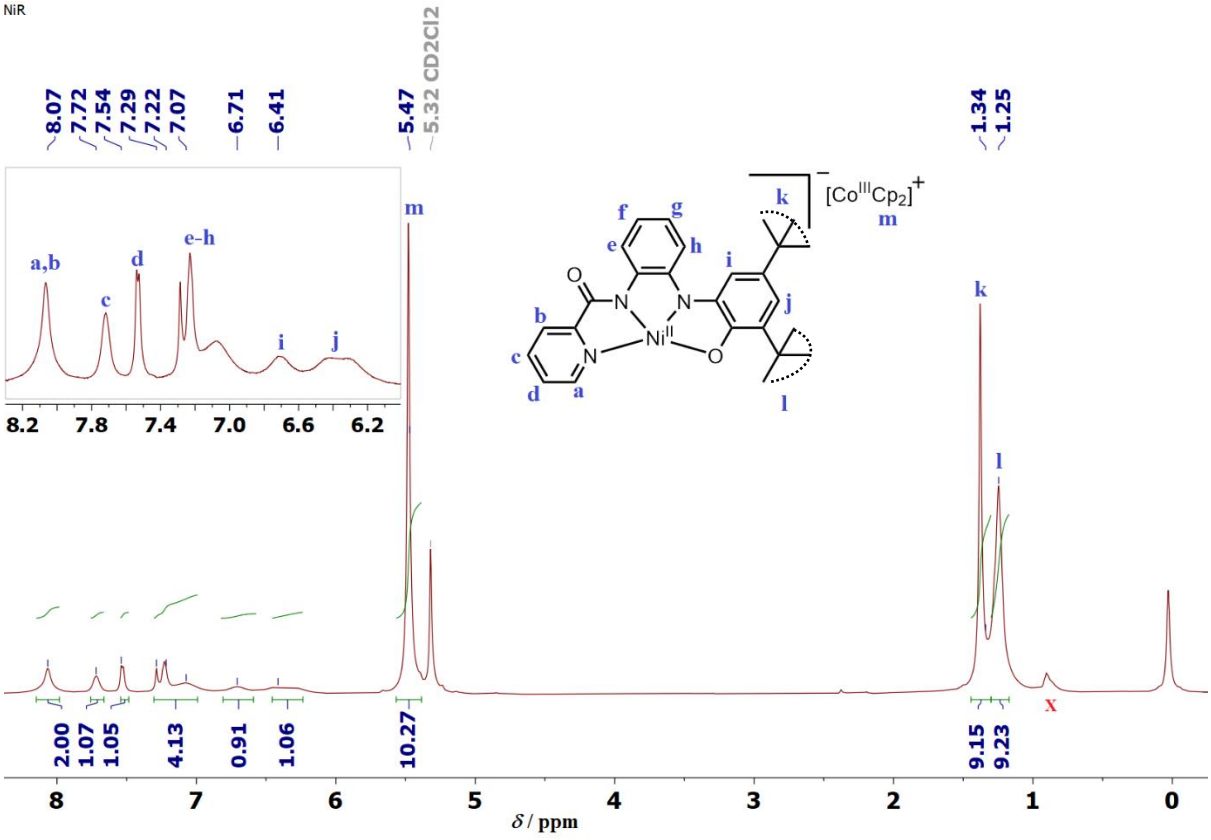

Fig. S11 ^{1}H NMR (CD_2Cl_2, 500 MHz) spectrum of $[Co(\eta^5\text{-}C_5H_5)_2][Ni(L^2)]$ **3**. x denotes impurity.

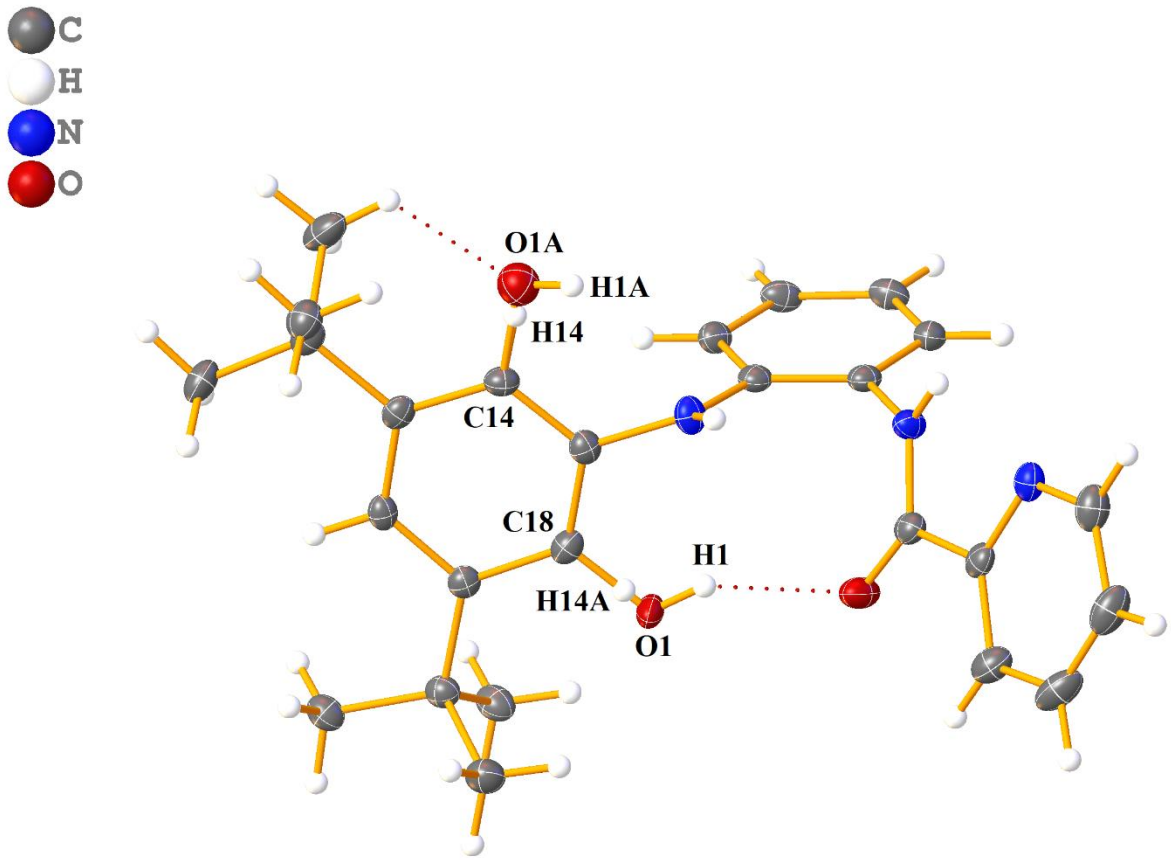

Fig. S12 Perspective view of H_3L^2 (with equivalent *meta*-positions disorder modelling). Only PART 1 and PART 2 atoms with corresponding carbon atoms are labelled. Modelled atoms in PART 1: O1, H1 and H14 and PART 2: O1A, H1A and H14A. The occupancy ratio of PART 1 and PART 2 is 90:10.

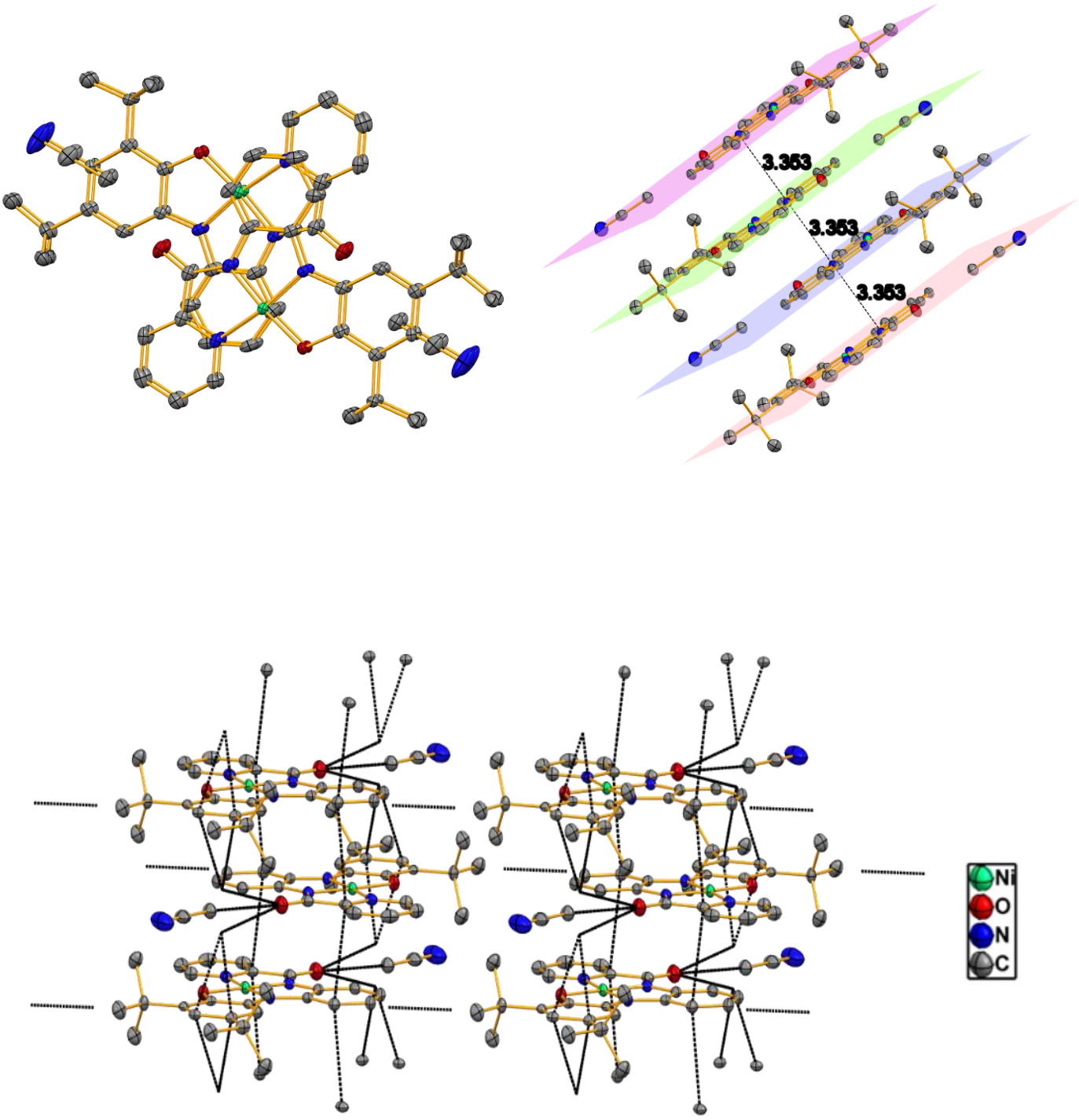

Fig. S13 Formation of alternating chains through π–π interactions in **1**•CH_3CN. The distance between two adjacent molecular planes is 3.353 Å.

(*a*)

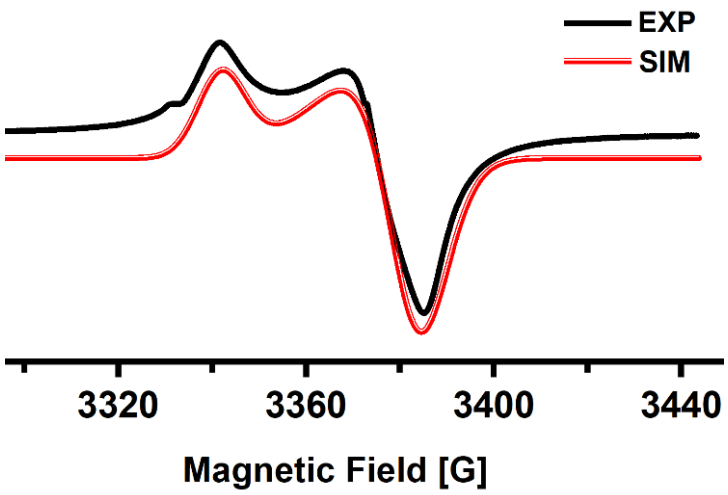

(*b*)

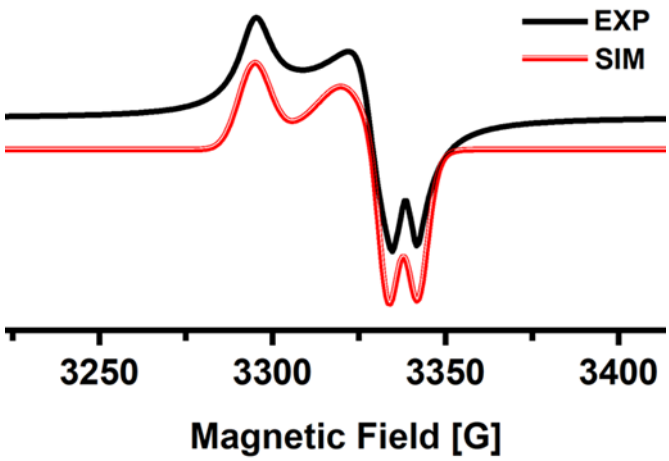

Fig. S14 X-band EPR spectrum (ν = 9.460 GHz, power = 0.201 mW, receiver gain = 1 x 10^2, modulation frequency = 100 KHz, modulation amplitude = 5.00 G) for **1** as solid recorded at (*a*) 300 K (upper trace); simulated spectrum (lower trace) with parameters: g_x = 1.995, g_y = 2.002, g_z = 2.020; $A^{Ni}_{(xx)}$ = 2 x 10^{-4} cm^{-1}; W_x = 18 G, W_y = 19 G, W_z = 15 G; (*b*) 80 K (upper trace); simulated spectrum (lower trace) with parameters: g_x = 1.995, g_y = 2.003, g_z = 2.021; $A^{H}_{(xx)}$ = 8 x 10^{-4} cm^{-1} , $A^{H}_{(yy)}$ = 7 x 10^{-4} cm^{-1}; W_x = 5 G, W_y = 14 G, W_z = 9 G. Error limits: $g \pm$ 0.002; $A \pm$ 0.0001 cm^{-1}; $W \pm 1$.

(*a*)

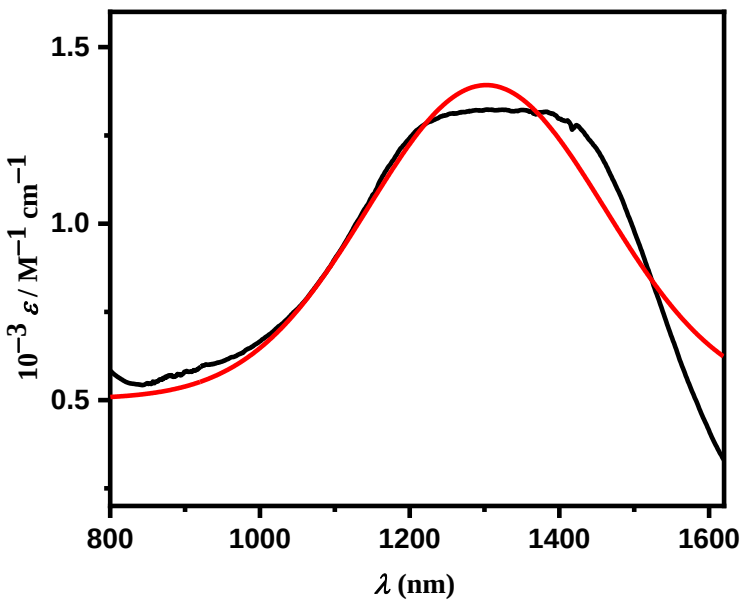

(*b*)

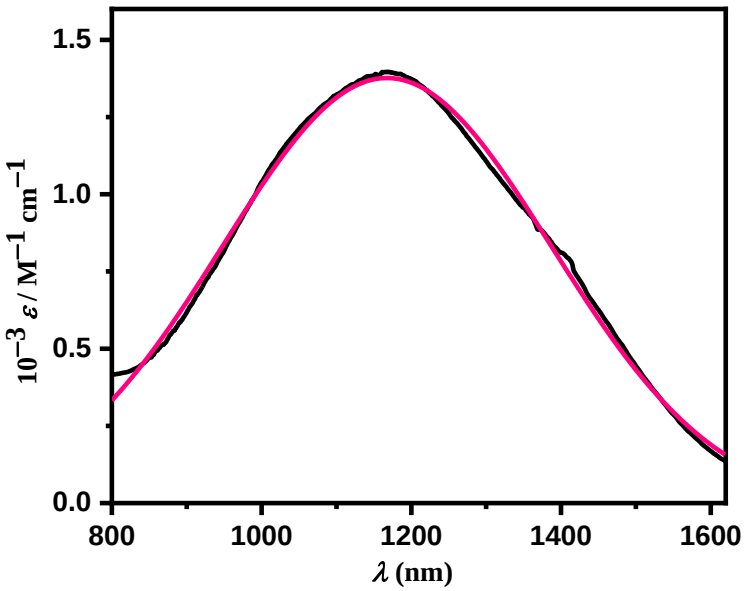

Fig. S15 NIR region plots (black) of (*a*) **1** and (*b*) **2** and their respective Gaussian-fit plots (red).

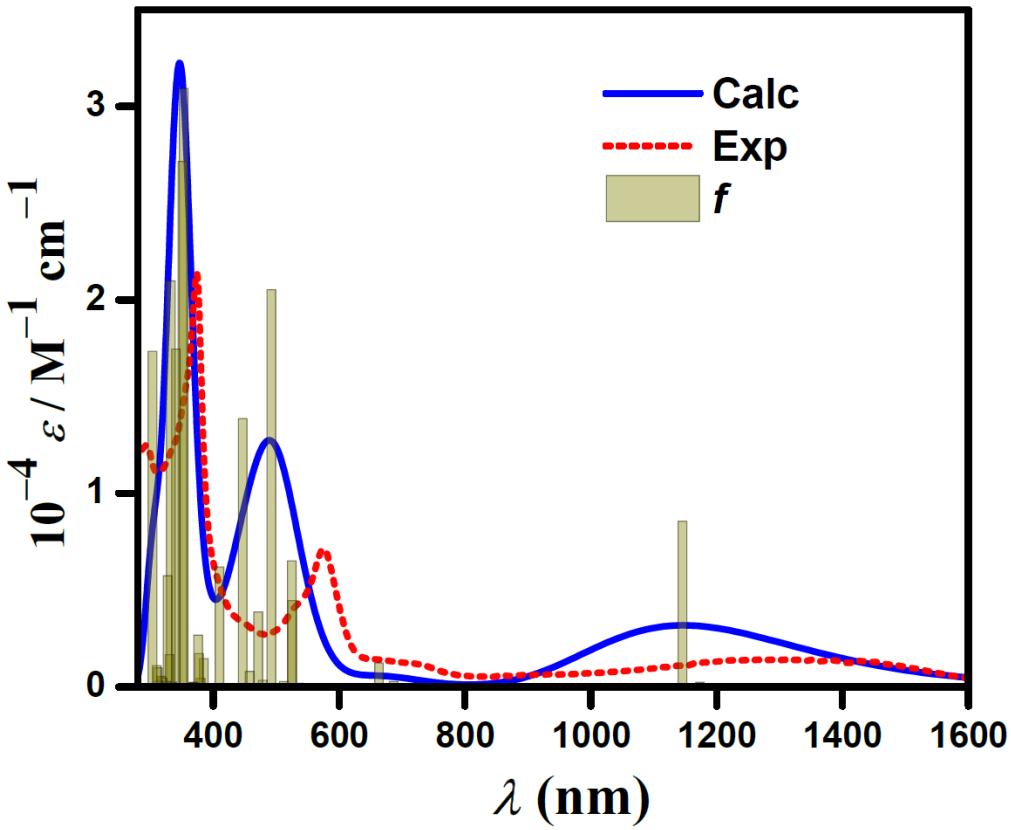

Fig. S16 TD-DFT-calculated electronic spectrum for $[Ni^{II}\{(L^2)^{\bullet 2-}\}]$ **1**.

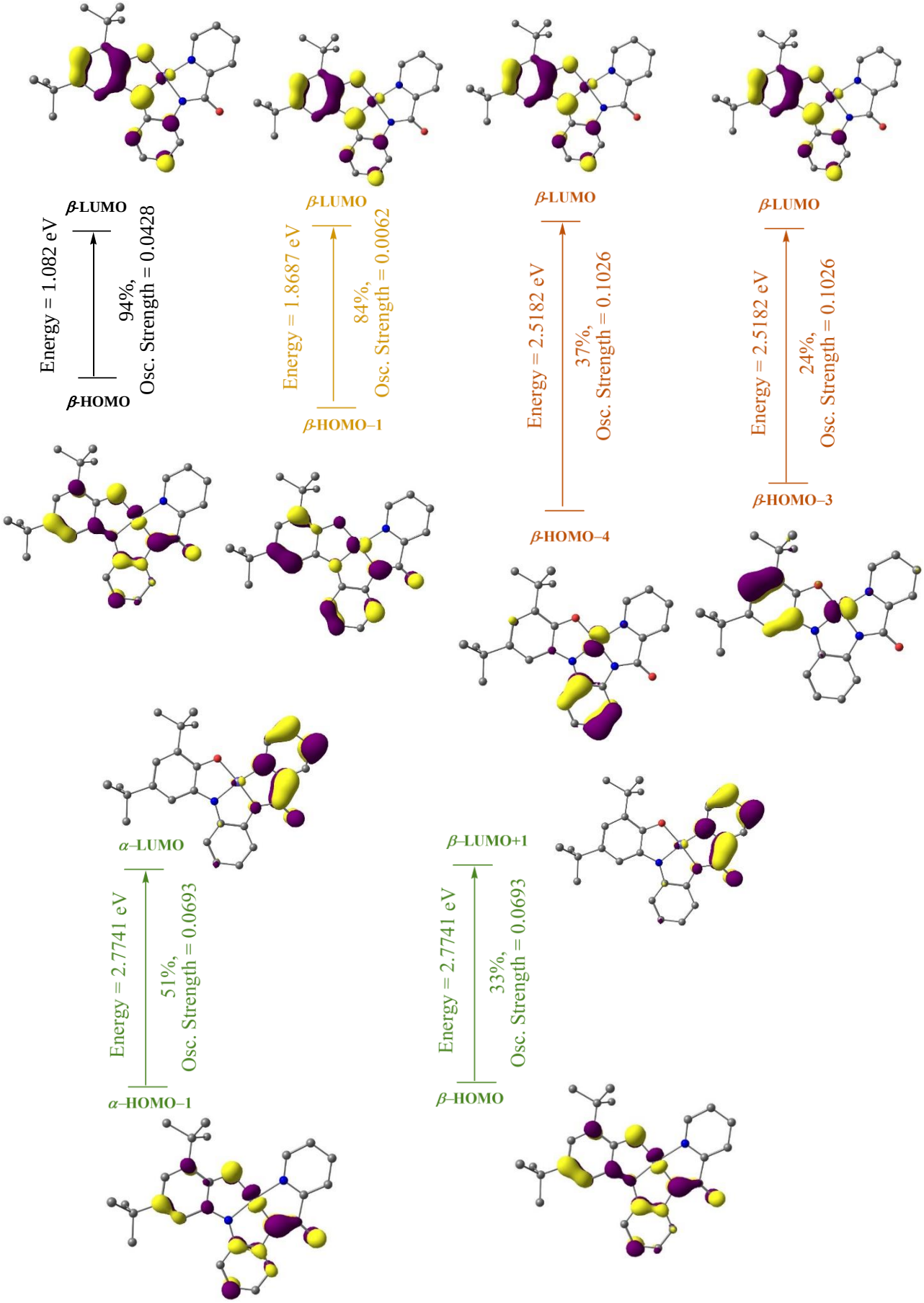
β-LUMO
Energy = 1.082 eV
94%,
Osc. Strength = 0.0428
β-HOMO
β-LUMO
Energy = 1.8687 eV
84%,
Osc. Strength = 0.0062
β-HOMO–1
β-LUMO
Energy = 2.5182 eV
37%,
Osc. Strength = 0.1026
β-HOMO–4
β-LUMO
Energy = 2.5182 eV
24%,
Osc. Strength = 0.1026
β-HOMO–3
α–LUMO
Energy = 2.7741 eV
51%,
Osc. Strength = 0.0693
α–HOMO–1
β–LUMO+1
Energy = 2.7741 eV
33%,
Osc. Strength = 0.0693
β–HOMO

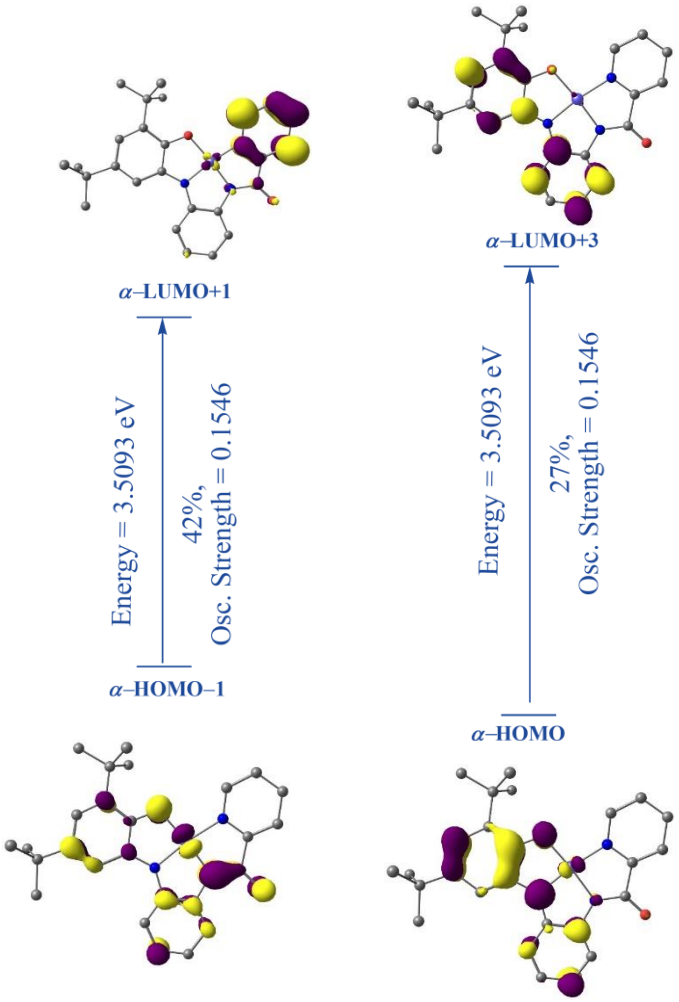

Fig. S17 Representative molecular-orbitals involved in TD-DFT transitions for $[Ni^{II}\{(L^2)^{\bullet 2-}]$ **1**.

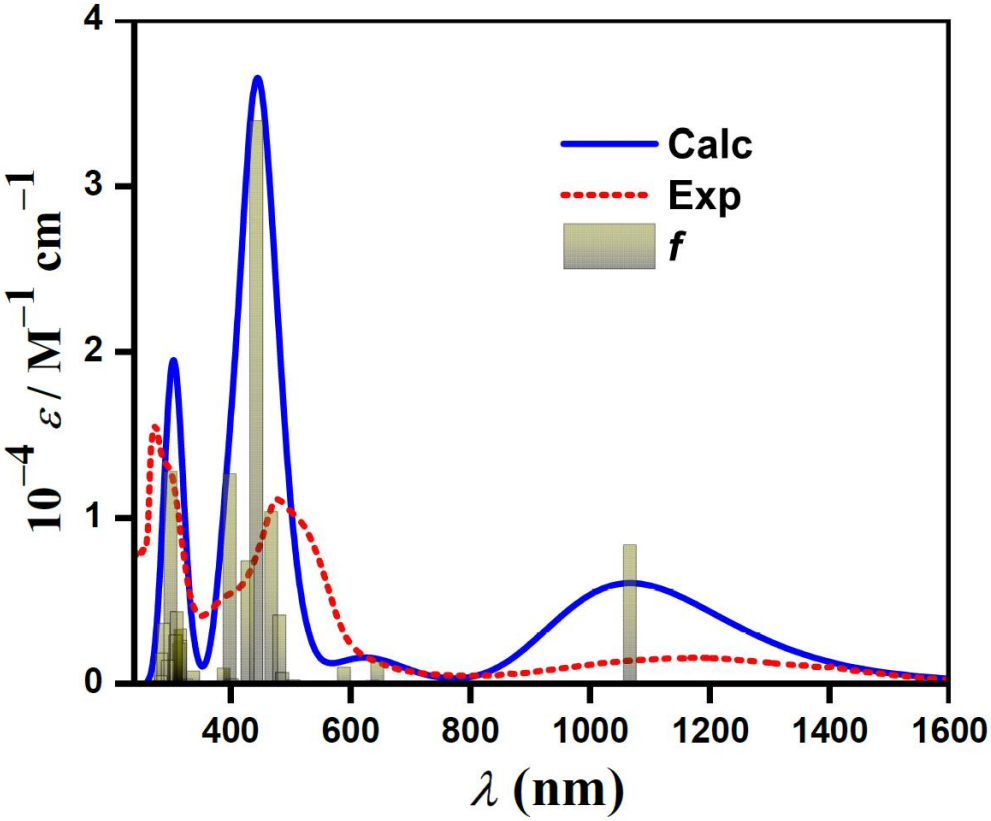

Fig. S18 TD-DFT-calculated electronic spectrum for $[Ni^{II}\{(L^2)^-\}]^+$ / $\mathbf{1}^+$.

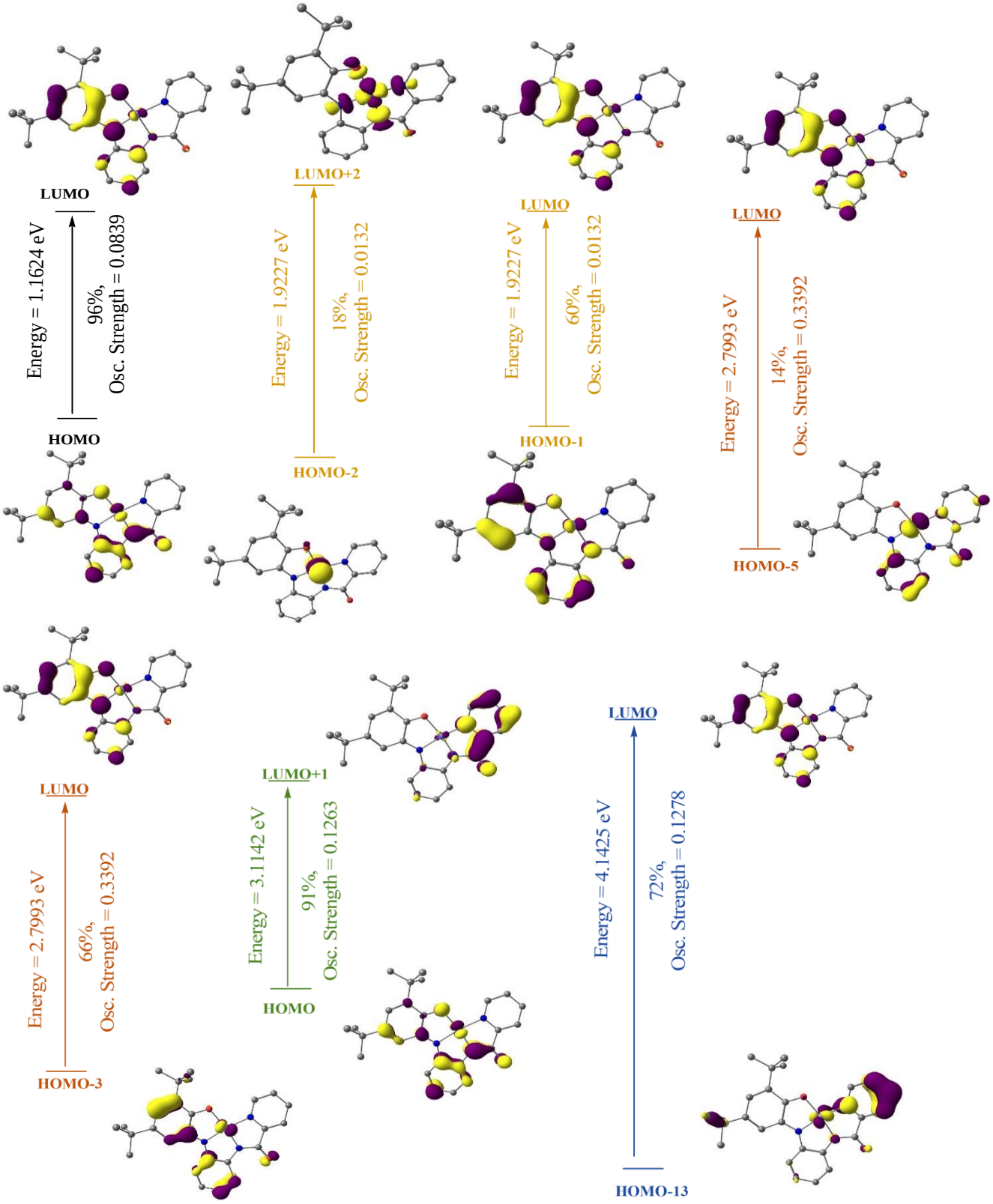

Fig. S19 Representative molecular-orbitals involved in TD-DFT transitions for $[Ni^{II}\{(L^2)^-\}]^+$/**1**$^+$.

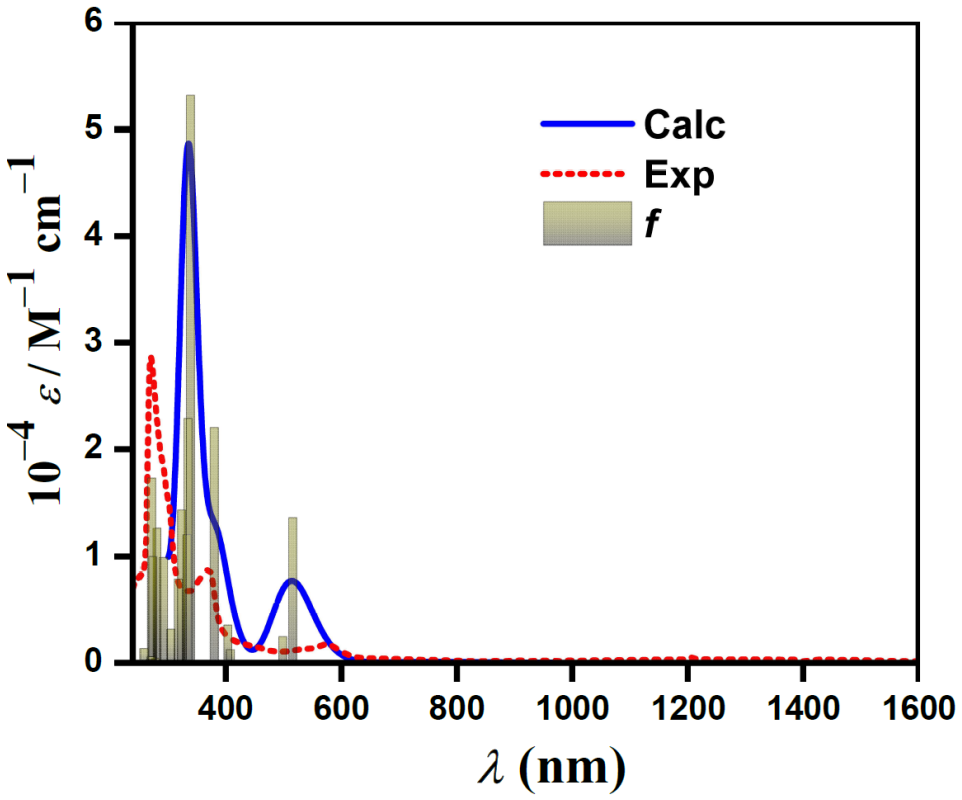

Fig. S20 TD-DFT calculated electronic spectrum for $[Ni^{II}\{(L^2)^{3-}\}]^-$ / **1**$^-$.

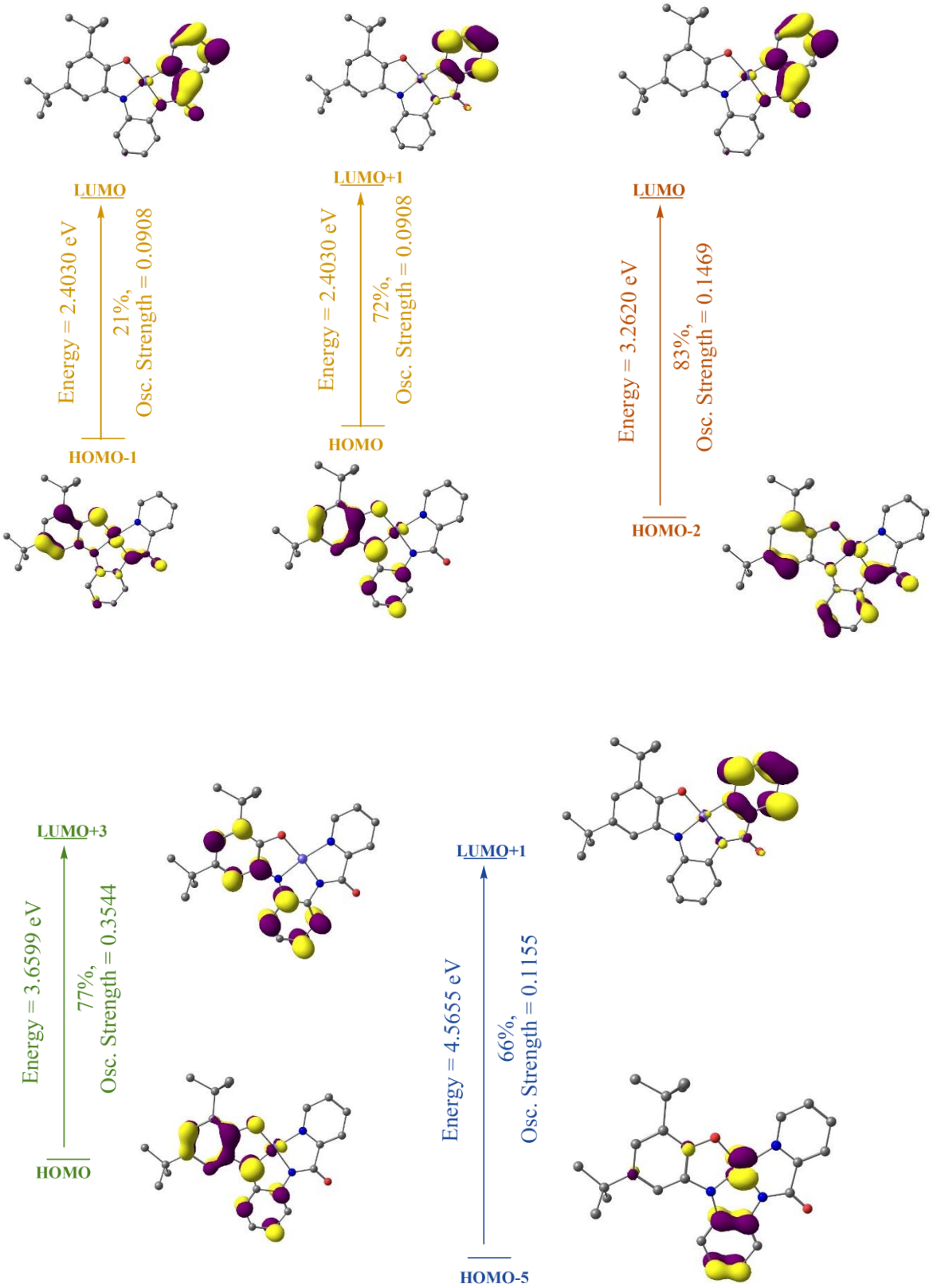

Fig. S21 Representative molecular-orbitals involved in TD-DFT transitions for $[Ni^{II}\{(L^2)^{3-}\}]^-$ / **1**$^-$.

Table S1 Data collection and structure refinement parameters for H_3L^2 and $[Ni(L^2)]\bullet CH_3CN$ (**1**•CH_3CN).

	H_3L^2	**1**•CH_3CN
Empirical formula	$C_{26}H_{31}N_3O_2$	$C_{28}H_{31}N_4NiO_2$
Formula weight	417.54	514.28
Crystal colour, habit	Light white, Block	Dark purple, Block
Temperature/K	100(10)	100(2)
Crystal system	Monoclinic	Orthorhombic
Space group	$P2_1/c$	*Pnma*
a/Å	12.8121(5)	13.2969(15)
b/Å	9.6447(4)	6.7069(8)
c/Å	18.5196(7)	27.780(3)
α/°	90.0	90.0
β/°	98.531(4)	90.0
γ/°	90.0	90.0
Volume/Å^3	2263.14(16)	2477.4(5)
Z	4	4
ρ_{calc} / gcm^{-3}	1.225	1.379
μ/mm^{-1}	0.078	0.816
F(000)	896.0	1084.0
Crystal size/mm^3	0.27 × 0.21 × 0.15	0.2 × 0.1 × 0.05
Radiation	Mo Kα (λ = 0.71073)	MoKα (λ = 0.71073)
Reflections measured	7644	29553
Unique reflections/ R_{int}	3977 (R_{int} = 0.0238)	2380 (R_{int} = 0.0832)
Reflections used [$I > 2\sigma(I)$]	3417	1897
Goodness-of-fit on F^2	1.069	1.059
Final R indexes [$I > 2\sigma(I)$]^{a,b}	R_1 = 0.0439, wR_2 = 0.1036	R_1 = 0.0327, wR_2 = 0.0689
Final R indexes [all data]^{a,b}	R_1 = 0.0513, wR_2 = 0.1083	R_1 = 0.0498, wR_2 = 0.0798

^{a} $R_1 = \Sigma||F_o| - |F_c||/\Sigma|F_o|$. ^{b} $wR_2 = \{\Sigma[w\,(|F_o|^2 - |F_c|^2)^2]/\Sigma[w(|F_o|^2)^2]\}^{1/2}$.

Table S2 Data collection and structure refinement parameters for $[Ni(L^2)](SbF_6)\bullet 0.5CH_2Cl_2$ (**2**•$0.5CH_2Cl_2$) and $[Co(\eta^5\text{-}C_5H_5)_2][Ni(L^2)]\bullet C_6H_6$ (**3**•C_6H_6).

	2•$0.5CH_2Cl_2$	**3**•C_6H_6
Empirical formula	$C_{26.50}H_{29}F_6N_3NiO_2SbCl$	$C_{42}H_{44}CoN_3NiO_2$
Formula weight	751.44	740.44
Crystal colour, habit	Dark red, Block	Brownish red, Block
Temperature/K	100(2)	100(1)
Crystal system	Triclinic	Triclinic
Space group	*P*-1	*P*-1
a/Å	8.0860(7)	10.6611(9)
b/Å	12.2357(10)	17.4758(15)
c/Å	15.7588(13)	19.0544(17)
α/°	67.728(3)	85.954(2)
β/°	81.980(3)	81.575(3)
γ/°	86.088(3)	89.811(3)
Volume/Å^3	1428.5(2)	3502.9(5)
Z	2	4
ρ_{calc} / *g* cm^3	1.747	1.404
μ/mm^{-1}	1.767	1.052
F(000)	750	1552.0
Crystal size/mm^3	0.2 × 0.1 × 0.05	0.2 × 0.1 × 0.05
Radiation	MoK$_\alpha$ (λ = 0.71073)	MoK$_\alpha$ (λ = 0.71073)
Reflections measured	11027	43863
Unique reflections/ R_{int}	5039 (R_{int} = 0.0290)	12386 (R_{int} = 0.0487)
Reflections used [$I > 2\sigma(I)$]	4526	10284
Goodness-of-fit on F^2	1.049	1.019
Final *R* indexes [$I > 2\sigma(I)$][a,b]	R_1 = 0.0246, wR_2 = 0.0566	R_1 = 0.0323, wR_2 = 0.0714
Final *R* indexes [all data][a,b]	R_1 = 0.0296, wR_2 = 0.0597	R_1 = 0.0438, wR_2 = 0.0779

[a] $R_1 = \Sigma||F_o| - |F_c||/\Sigma|F_o|$. [b] $wR_2 = \{\Sigma[w\,(|F_o|^2 - |F_c|^2)^2]/\Sigma[w(|F_o|^2)^2]\}^{1/2}$.

Table S3 Selected Bond angles for $[Ni(L^2)]\bullet CH_3CN$ (**1**), $[Ni(L^2)](SbF_6)\bullet 0.5CH_2Cl_2$ (**2**•$0.5CH_2Cl_2$) and $[Co(\eta^5\text{-}C_5H_5)_2][Ni(L^2)]\bullet C_6H_6$ (**3**•C_6H_6) in (˚**).**

Bond angles	**1**	**2**	**3**
N1–Ni–O1	100.54(10)	101.03(9)	99.92(7)
N1–Ni–N2	85.28(12)	85.94(9)	85.45(8)
N1–Ni–N3	171.86(11)	173.00(9)	172.02(8)
N2–Ni–N3	86.59(11)	87.05(9)	86.67(8)
N2–Ni–O1	174.18(11)	172.86(9)	174.61(8)
N3–Ni–O1	87.59(10)	85.97(8)	87.97(7)

Table S4 DFT-optimised cartesian coordinates for $[Ni(L^2)]$.

Ni	1.942910000	8.900680000	8.251783000
O	2.234378000	9.743049000	9.901352000
O	2.022459000	6.473806000	5.123462000
N	0.702996000	10.230936000	7.907074000
N	3.147934000	7.414820000	8.368982000
N	1.513633000	8.220450000	6.590700000
C	0.511842000	12.626880000	11.271481000
H	0.487084000	13.253787000	12.161209000
C	0.529838000	11.084046000	8.957994000
C	1.436591000	10.774023000	10.050499000
C	-0.417891000	12.929224000	10.232393000

C	-0.396655000	12.151050000	9.087689000
H	-1.106447000	12.340868000	8.292352000
C	1.430786000	11.585306000	11.230670000
C	3.104630000	6.638815000	7.259563000
C	0.575668000	8.986475000	5.906803000
C	0.127983000	10.138416000	6.644731000
C	3.861306000	11.393367000	11.898552000
H	4.058661000	10.685774000	11.082728000
H	4.557805000	11.175613000	12.725457000
H	4.081300000	12.409389000	11.532660000
C	3.898098000	5.502193000	7.135226000
H	3.820878000	4.915568000	6.218539000
C	2.398921000	11.294266000	12.394985000
C	2.143863000	7.093577000	6.179516000
C	3.965241000	7.097414000	9.380545000
H	3.942684000	7.769677000	10.239855000
C	0.079547000	8.731335000	4.620767000
H	0.428230000	7.848329000	4.088005000
C	4.754722000	5.164380000	8.185908000
H	5.390230000	4.278132000	8.117880000
C	-1.402296000	14.097701000	10.427847000
C	-0.782027000	11.023232000	6.028794000
H	-1.105124000	11.930758000	6.530151000
C	2.126958000	9.879178000	12.959798000
H	1.100900000	9.807756000	13.355512000
H	2.822989000	9.660177000	13.786772000
H	2.249875000	9.107690000	12.188527000
C	4.789523000	5.972851000	9.325208000
H	5.445244000	5.742010000	10.166396000
C	2.230051000	12.298550000	13.550698000
H	2.432572000	13.333903000	13.233896000
H	2.943738000	12.055519000	14.353497000

H	1.220072000	12.263354000	13.988760000
C	-0.838394000	9.616228000	4.050261000
H	-1.222185000	9.417767000	3.046469000
C	-1.258324000	10.758379000	4.745870000
H	-1.960988000	11.454643000	4.282116000
C	-2.283605000	13.829073000	11.670453000
H	-2.868705000	12.904031000	11.546160000
H	-2.989847000	14.660846000	11.828981000
H	-1.683749000	13.724800000	12.587309000
C	-0.609342000	15.410043000	10.634288000
H	0.044195000	15.363692000	11.518640000
H	-1.299707000	16.257815000	10.776835000
H	0.024426000	15.629487000	9.760401000
C	-2.330296000	14.285732000	9.214343000
H	-1.764889000	14.508642000	8.295837000
H	-3.013047000	15.130969000	9.393684000
H	-2.950900000	13.394960000	9.029213000

Table S5 DFT-optimised cartesian coordinates for $[Ni(L^2)]^+$ / $\mathbf{1}^+$

Ni	2.183333000	4.332201000	7.640939000
O	2.770832000	5.114762000	9.272622000
O	0.356678000	2.294686000	4.795529000
N	3.513455000	5.374930000	6.829427000
N	1.799455000	3.715162000	5.951176000
N	0.753668000	3.208019000	8.209200000
C	3.625540000	5.142836000	5.477009000
C	3.523876000	4.461300000	2.758630000
H	3.495624000	4.212479000	1.694937000
C	2.581537000	3.901307000	3.607356000
H	1.817685000	3.217482000	3.242349000
C	2.626488000	4.214797000	4.982615000

C	0.171784000	2.545302000	7.178288000
C	4.126433000	6.212469000	7.673892000
C	0.765052000	2.817090000	5.817622000
C	3.680658000	5.988782000	9.073649000
C	0.301984000	3.034022000	9.459515000
H	0.814057000	3.594877000	10.242501000
C	4.590295000	5.668750000	4.575896000
H	5.397014000	6.305466000	4.926634000
C	5.618683000	7.980745000	8.399801000
C	4.535250000	5.329443000	3.239096000
H	5.282975000	5.723967000	2.548683000
C	5.075293000	7.240452000	7.381862000
H	5.333361000	7.459271000	6.353375000
C	-0.895819000	1.677540000	7.376455000
H	-1.326623000	1.170954000	6.511103000
C	3.887891000	6.510922000	11.616175000
C	5.217377000	7.684889000	9.764519000
H	5.687161000	8.278799000	10.546144000
C	4.287708000	6.747116000	10.147412000
C	6.621213000	9.117388000	8.167464000
C	-0.765010000	2.177906000	9.731978000
H	-1.108602000	2.056913000	10.760502000
C	-1.372350000	1.491083000	8.677309000
H	-2.209732000	0.815898000	8.867226000
C	6.023674000	10.437916000	8.714137000
H	5.086716000	10.695826000	8.196195000
H	6.736443000	11.262136000	8.555788000
H	5.814068000	10.391476000	9.793623000
C	7.937515000	8.791241000	8.916113000
H	7.793010000	8.693045000	10.002762000
H	8.665454000	9.601868000	8.756902000
H	8.385517000	7.855721000	8.546283000

C	4.179926000	5.041559000	12.007948000
H	3.606419000	4.327763000	11.401868000
H	3.912908000	4.880780000	13.064057000
H	5.250710000	4.808175000	11.896177000
C	2.384544000	6.829040000	11.806506000
H	2.168264000	7.879831000	11.556505000
H	2.103694000	6.672096000	12.859781000
H	1.743270000	6.189063000	11.186116000
C	4.687247000	7.420483000	12.567590000
H	5.771695000	7.237372000	12.506609000
H	4.381630000	7.218168000	13.604652000
H	4.501811000	8.489424000	12.377894000
C	6.943117000	9.308672000	6.675584000
H	7.403373000	8.410438000	6.234107000
H	7.661224000	10.133083000	6.554969000
H	6.047976000	9.569779000	6.089221000

Table S6 DFT-optimised cartesian coordinates for $[Ni(L^2)]^-$ / **1**$^-$

Ni	8.086004000	1.101184000	18.239649000
O	6.394456000	0.377681000	17.977872000
N	7.281052000	2.466035000	19.163180000
N	9.167348000	-0.202290000	17.337986000
N	9.697621000	1.951768000	18.595826000
O	12.009972000	1.754932000	18.246961000
C	8.159776000	3.423656000	19.630989000
C	5.451829000	1.131967000	18.565153000
C	5.900818000	2.315278000	19.252081000
C	7.888075000	4.612537000	20.341448000
H	6.866660000	4.891828000	20.584353000
C	8.928776000	5.465235000	20.736999000
H	8.680227000	6.378731000	21.287087000

C	3.586562000	2.816859000	19.886378000
C	10.486075000	0.107702000	17.400346000
C	4.962129000	3.125661000	19.903456000
H	5.297015000	4.007560000	20.441647000
C	4.077648000	0.808066000	18.534618000
C	9.540669000	3.141419000	19.322946000
C	10.259576000	5.169456000	20.440804000
H	11.062604000	5.841393000	20.756734000
C	11.451778000	-0.708178000	16.814914000
H	12.496118000	-0.403938000	16.900270000
C	10.565251000	3.999909000	19.726183000
H	11.591999000	3.739687000	19.470749000
C	3.589386000	-0.457691000	17.795796000
C	3.176100000	1.669257000	19.200997000
H	2.118118000	1.421277000	19.178699000
C	10.828260000	1.386741000	18.141219000
C	2.599909000	3.749847000	20.621623000
C	11.044191000	-1.869101000	16.150647000
H	11.780633000	-2.527589000	15.681998000
C	8.769807000	-1.311973000	16.704262000
H	7.692169000	-1.487587000	16.701627000
C	9.682138000	-2.176107000	16.094086000
H	9.320755000	-3.072340000	15.585696000
C	2.060696000	-0.633933000	17.871952000
H	1.708166000	-0.736724000	18.910633000
H	1.766464000	-1.548214000	17.329119000
H	1.523187000	0.211660000	17.413806000
C	3.974762000	-0.372604000	16.299605000
H	3.474981000	0.485426000	15.820092000
H	3.665909000	-1.288585000	15.763585000
H	5.059370000	-0.242742000	16.186371000
C	4.234831000	-1.714391000	18.427113000

H	5.330275000	-1.640940000	18.401302000
H	3.924265000	-2.626918000	17.886165000
H	3.923256000	-1.821459000	19.479410000
C	1.139488000	3.277093000	20.499415000
H	0.471606000	3.970872000	21.037612000
H	0.997290000	2.274094000	20.931369000
H	0.808858000	3.242243000	19.449482000
C	2.684135000	5.176683000	20.030269000
H	2.418788000	5.170798000	18.960770000
H	3.699948000	5.591358000	20.114463000
H	1.994271000	5.863711000	20.552572000
C	2.953017000	3.806704000	22.126694000
H	2.265421000	4.479656000	22.669956000
H	3.978587000	4.171168000	22.289452000
H	2.883712000	2.805213000	22.581275000

Table S7 DFT-calculated metric parameters for 1, 1^+ and 1^-.

	1	**1^+**	**1^-**
Ni–O1	1.852(2) [1.8750]	1.871(2) [1.9026]	1.842(2) [1.8583]
Ni–N1	1.885(3) [1.9166]	1.875(2) [1.9054]	1.881(2) [1.9168]
Ni–N2	1.826(3) [1.8456]	1.817(2) [1.8394]	1.826(2) [1.8567]
Ni–N3	1.822(3) [1.8509]	1.851(2) [1.8748]	1.814(2) [1.8343]
C1–C2	1.391(4) [1.3954]	1.382(4) [1.3948]	1.381(3) [1.3969]
C2–C3	1.387(5) [1.3974]	1.387(4) [1.3974]	1.383(3) [1.3973]

C3–C4	1.382(5) [1.3971]	1.384(4) [1.3978]	1.394(3) [1.3982]
C4–C5	1.379(4) [1.3917]	1.377(4) [1.3899]	1.377(3) [1.3931]
C5–C6	1.506(5) [1.5153]	1.503(4) [1.5090]	1.515(3) [1.5172]
C7–C8	1.397(4) [1.4018]	1.396(4) [1.4112]	1.385(3) [1.3962]
C8–C9	1.386(5) [1.3968]	1.386(4) [1.3863]	1.395(3) [1.4042]
C9–C10	1.386(5) [1.4016]	1.393(4) [1.4168]	1.386(3) [1.3950]
C10–C11	1.394(5) [1.3938]	1.383(4) [1.3803]	1.392(3) [1.4023]
C11–C12	1.399(4) [1.4108]	1.409(4) [1.4210]	1.403(3) [1.4113]
C7–C12	1.430(4) [1.4394]	1.429(3) [1.4504]	1.429(3) [1.4427]
C13–C14	1.404(4) [1.4190]	1.427(4) [1.4291]	1.393(3) [1.4007]
C14–C15	1.377(4) [1.3843]	1.364(4) [1.3709]	1.401(3) [1.4099]
C15–C16	1.418(4) [1.4267]	1.454(4) [1.4529]	1.390(3) [1.3982]
C16–C17	1.381(4) [1.3896]	1.351(4) [1.3748]	1.412(3) [1.4136]
C17–C18	1.416(4) [1.4321]	1.450(3) [1.4479]	1.398(3) [1.4121]
C13–C18	1.442(4) [1.4532]	1.493(4) [1.4859]	1.432(3) [1.4403]
C1–N1	1.341(4) [1.3386]	1.333(3) [1.3407]	1.338(3) [1.3383]
C5–N1	1.358(4) [1.3545]	1.367(3) [1.3566]	1.358(3) [1.3561]
C6–N2	1.352(4) [1.3550]	1.364(3) [1.3763]	1.351(3) [1.3432]
C7–N2	1.395(4) [1.3908]	1.396(3) [1.3681]	1.412(3) [1.4030]

C12–N3	1.395(4) [1.3908]	1.401(3) [1.3767]	1.391(3) [1.3813]
C13–N3	1.371(4) [1.3646]	1.339(3) [1.3380]	1.389(3) [1.3912]
C18–O1	1.323(4) [1.3121]	1.263(3) [1.2772]	1.353(2) [1.3425]
C6–O2	1.228(4) [1.2305]	1.228(3) [1.2183]	1.232(3) [1.2422]

Table S8 TD-DFT-calculated electronic transitions of [$Ni^{II}(L^2)$]

Excitation energy(eV)	λ (nm)	f	Transition	Character
1.0822	1145	0.0428	β–H [~84%L] → β –L [~95%L] (94%)	CT involving amidato part→ phenyl-iminosemiquinonate part CT involving phenylenediamide → phenyl-iminosemiquinonate part MLCT involving Ni → phenyl-iminosemiquinonate part
1.8687	663	0.0062	β–H–1 [~86%L] → β –L [~95%L] (84%)	CT involving amidato part→ phenyl-iminosemiquinonate part CT involving phenylenediamide → phenyl-iminosemiquinonate part MLCT involving Ni → phenyl-iminosemiquinonate part
2.5182	492	0.1026	β–H–4 [~59%L] → β –L [~95%L] (37%) β-H–3 [~59%L] → β –L [~95%L] (24%)	MLCT involving Ni→ phenyl-iminosemiquinonate part CT involving phenylenediamide → phenyl-iminosemiquinonate part CT involving phenyl-iminosemiquinonate ring → phenylenediamide MLCT involving Ni → phenyl-iminosemiquinonate part
2.7741	446	0.0693	α–H–1 [~80%L] → α –L [~98%L] (51%)	CT involving phenylenediamide → pyridine CT involving phenyl-iminosemiquinonate part → pyridine MLCT involving Ni → pyridine

			β–H [~84%L] → β –L+1 [~98%L] (33%)	CT involving phenylenediamide → pyridine CT involving phenyl-iminosemiquinonate part → pyridine MLCT involving Ni → pyridine
3.5093	353	0.1546	α–H–1[~80%L] → α –L+1[~98%L] (42%)	CT involving amidato → pyridine CT involving phenylenediamide → pyridine CT involving phenyl-iminosemiquinonate part → pyridine MLCT involving Ni → pyridine
			α–H[~95%L] → α –L+3[~99%L] (27%)	CT in phenyl-iminosemiquinonate part and phenylenediamide and minor MLCT involving Ni → phenylenediamide

[a]H and L stands for KS-HOMO and KS-LUMO, respectively

[b]CT and MLCT stands for charge transfer and metal-to-ligand chanrge transfer, respectively

Table S9 TD-DFT-calculated electronic transitions of $[Ni^{II}(L^2)]^+$

Excitation energy(eV)	λ (nm)	f	Transition	Character
1.1624	1066	0.0839	H [~88%L] → L [~96%L] (96%)	CT involving amidato and phenylenediamide →phenyl iminoquinone part and minor MLCT involving Ni → phenyl-iminoquinone part
1.9227	644	0.0132	H–2 [~87%M] → L+2 [~57%L] (18%)	MLCT involving Ni → pyridine, amidato and phenyl-iminoquinone part
			H–1 [~93%L] → L [~96%L] (60%)	CT involving amidato → phenyl-iminoquinone part CT in phenyl-iminoquinone part CT involving phenylenediamide → phenyl-iminoquinone part
2.7993	442	0.3392	H–5 [~54%M] → L [~96%L] (14%)	CT involving amidato → phenyl-iminoquinone part MLCT involving Ni → phenyl-iminoquinone part
			H–3 [~83%L] → L [~96%L] (66%)	CT in phenyl-iminoquinone part and phenylenediamide minor MLCT involving Ni →phenyl-iminoquinone part
3.1142	398	0.1263	H [~88%L] → L+1 [~98%L] (91%)	CT involving phenyl-iminoquinone, phenylenediamide and amidato → pyridine and minor MLCT involving Ni → pyridine

4.1425	299	0.1278	H−13 [~85%L] → L [~96%L] (72%)	CT involving pyridine → phenyl-iminoquinone part and phenylenediamide and minor MLCT involving Ni → phenyl-iminoquinone part

[a]H and L stands for KS-HOMO and KS-LUMO, respectively

[b]CT and MLCT stands for charge transfer and metal-to-ligand chanrge transfer, respectively.

Table S10 TD-DFT-calculated electronic transitions of $[Ni^{II}(L^2)]^-$

Excitation energy(eV)	λ (nm)	f	Transition	Character
2.4030	515	0.0908	H–1 [~82%L] → L [~98%L] (21%)	CT involving amidophenolate → pyridine and minor MLCT involving Ni → pyridine
			H [~94%L] → L+1 [~98%L] (72%)	CT involving amidophenolate and phenylenediamide → pyridine
3.2620	380	0.1469	H–2 [~87%L] → L [~98%L] (85%)	CT involving phenylenediamide , amidato and amidophenolate → pyridine and minor MLCT involving Ni → pyridine
3.6599	338	0.3544	H [~94%L] → L+3 [~99%L] (77%)	CT involving phenylenediamide → amidophenolate
4.5655	271	0.1155	H–5 [~60%M] → L+1 [~99%L] (66%)	MLCT involving Ni → pyridine CT involving phenylenediamide → pyridine

[a]H and L stands for KS-HOMO and KS-LUMO, respectively

[b]CT and MLCT stands for charge transfer and metal-to-ligand chanrge transfer, respectively.